EEG Source Analysis with a Finite-Element-based Convolutional Neural Network - feCNN

Athanasios Delatolas[1] adelatolas@tuc.gr

Marios Antonakakis[1] mantonakakis@isc.tuc.gr

Carsten H. Wolters[2,3] carsten.wolters@uni-muenster.de

Michalis Zervakis[1] michalis@display.tuc.gr

[1]School of Electrical and Computer Engineering
Technical University of Crete, Greece

[2]Institute for Biomagnetism and Biosignalanalysis
[3]Otto Creutzfeldt Center for Cognitive and Behavioral Neuroscience
University of Münster, Münster, Germany

***Abstract*—To reconstruct the electrophysiological activity of brain responses, source analysis is performed through the solution of the forward and inverse problems. The former contains a unique solution while the latter is ill-posed. In this regard, many algorithms have been suggested relying on different prior information for solving the inverse problem. Recently, deep convolutional neural networks (CNN) have been used to deal with source analysis. However, their underlying training for inverse solutions suboptimal forward modeling. In this work, we proposed a finite-element-based CNN, the feCNN, for which, training is applied on the basis of skull-conductivity calibrated and white matter anisotropic head modeling. We first show the performance of feCNN using simulated data while a realistic application on somatosensory evoked potentials follows. A comparison is presented including well-known inverse solutions. The throughput of feCNN can potentially pave the way for real-time applications using realistic head modeling.**

***Index Terms*—source analysis; convolutional neural networks; FEM; EEG; somatosensory evoked responses**

I. Introduction

To perform Electroencephalography (EEG) or Magnetoencephalography (MEG) source analysis, we need to solve the forward problem which relies on the flow-estimation of the electric field to the EEG or MEG sensors for a given brain source. The next problem is the estimation of an inverse solution for which we reconstruct the neuronal activity given the original EEG or MEG data and the forward solution on the basis of a three-dimensional geometry of the head.

The EEG/MEG forward solution has been proved to be unique [3]. The most commonly used numerical techniques that solve the forward problem are the Bounded Element Method (BEM) [4], Finite Element Method (FEM) [5]. In this study, we opted for FEM because of its high flexibility to accurately model the electromagnetic field propagation in geometrically challenging inhomogeneous and anisotropic head volume conductors such as the human head [3].

During the inverse solution, an endless number of source and parameter configurations can yield the same EEG/MEG measurements, characterizing the EEG/MEG inverse problem as ill-posed [2]. A wide range of inverse reconstructions based on various a priori assumptions have been created. These reconstructions are broadly classified as equivalent current dipole, current density reconstruction, beamforming, and hierarchical Bayesian modeling [3]. In this work, Single Dipole Scan [14] and sLORETA [15] are used for source localization evaluations additionally to our proposed solution.

These two source localization techniques have been evaluated [2], but a prior knowledge is important making the problem laborious posing also problems for real-time applications. Recently, Deep Learning methods have been proposed to overcome these limitations. A Multi-Layer Perceptron(MLP) network [9] and various CNNs such as [7], [8]. Deep Learning has the potential to offer real-time source localization. However, in these methods, no accurate and realistic head modeling is used which can potentially lead to suboptimal source reconstructions.

In this work, we propose a new finite-element-based Convolutional Neural Network (feCNN) architecture for source reconstruction of somatosensory evoked potentials. We first create a number of simulated brain source signals using an individually skull-conductivity calibrated and white-matter conductivity anisotropic head model. For the specific head model, finite elements (geometrically adapted hexahedrons) are used. We then train our proposed CNN with input the scalp topographies of the simulated data and evaluate its performance with the localization error for different levels of noise. Finally, we test our trained model with real somatosensory evoked responses for the localization of the P20/N20 component.

II. Methods

A. EEG forward problem

The forward problem is concerned with the computation of the channels measurements $\mathbf{M} \in \mathbb{R}^N$ given the moments (magnitude and orientation) $\mathbf{D} \in \mathbb{R}^p$ of the dipoles. Thus, it can be expressed mathematically over time as [2]:

$$\mathbf{M} = \mathbf{GD} + \mathbf{n} \tag{1}$$

where $\mathbf{M} \in \mathbb{R}^{N\times t}$, $\mathbf{G} \in \mathbb{R}^{N\times p}$ is the leadfield matrix which describes the flow of electrical current of each dipole through every electrode, $\mathbf{D} \in \mathbb{R}^{p\times t}$, and $\mathbf{n}$ is the noise of the recording system.

Moreover, the EEG electrodes are located on the scalp while the dipoles are inside the head. Therefore, a head model is required which is a simulation of the geometrical and electromagnetic features of the head. We utilized a six-compartment head model [1]. The compartments and their isotropic conductivites are: skin $0.43\ S/m$, skull compacta $0.31\ S/m$, skull spongiosa $0.01116\ S/m$, cerebrospinal fluid (CSF) $1.79\ S/m$, white and gray matter. The anisotropic conductivity tensors for the compartments gray and white matter were determined in [1].

Based on the above-mentioned head model, a source space with 50460 dipoles was created in [1]. The dipoles were placed 2 mm far-away from the neighbor compartment (i.e., skull compacta or CSF) to fulfill the so-called "St. Venant" condition [1]. Because our neural network could not converge with this extremely detailed source space, we downsampled it to $p = 10,092$ dipoles. A source space with $10,092$ sources is still more accurate than the ones that have been used in the latest Deep Learning studies [7], [8], [9]. Moreover, we used an EEG recording system with $N = 74$ electrodes.

Finally, we utilized DUNEuro [6] in order to calculate the leadfield matrix and thereby solve the forward problem with the Finite Element Method (FEM).

B. Simulation of EEG snapshots

Having solved the forward problem, we can now proceed to the solution of the inverse problem, that is, to estimate the most possible source activity which could generate the scalp EEG recordings. Since the inverse problem is solved using a neural network, we must generate the training dataset. To train a deep learning model and evaluate its performance, we need to know the exact location and moment of the underlying neural sources that give rise on the EEG data.

Our neural network is designed to operate on single time instances of EEG data with a single source. Thus, we simulate the electrical activity as described in [7]. In particular, each simulation had one dipole cluster, which can be thought as a smooth area of brain activity. A dipole cluster was created by randomly selecting a dipole in the source space and then applying a region growing approach. Starting from a single seeding dipole, we recursively incorporated all surrounding neighbors, resulting in a bigger source extent with each iteration. The seed dipole was assigned to an amplitude between 5 and 10 Nano-Ampere Meters (nAm). The amplitude of adjacent dipoles were attenuated based on their distance from the seed dipole. The attenuation followed a Gaussian distribution $\mathcal{N}(0, \frac{\text{distance\_from\_seed}}{2})$.

The simulated electric activation $\mathbf{D} \in \mathbb{R}^p$ of $p = 10,092$ dipoles was then projected to the leadfield matrix $\mathbf{G} \in \mathbb{R}^{N \times p}$ in order to calculate the potentials at the 74 EEG electrodes $\mathbf{M} \in \mathbb{R}^N$ placed on the scalp. We now differ from the approach of [7] and simulate the potentials of the EEG-electrodes with the following procedure. To generate realistic training data, we added Gaussian white noise at a specific signal-to-noise ratio (SNR) level. The SNR is set based on the power of the neural sources to be 15 dB:

$$\text{SNR} = 10 \cdot \log\left(\frac{P_{\text{signal}}}{P_{\text{noise}}}\right) \tag{2}$$

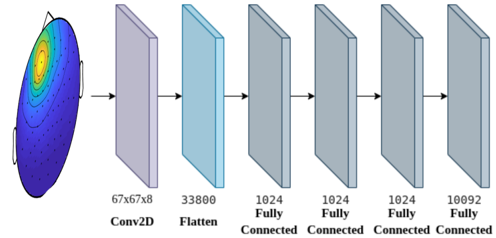

Fig. 1: The feCNN architecture

where P_{signal} is the power of the simulated electric activation and P_{noise} is the power of the additive Gaussian noise (unknown variable in the above equation). Finally, from the simulated 74 channel measurements we create their topography using FieldTrip [10]. With the aforementioned algorithm, a set of $100,000$ training samples (electrical currents of neural sources and their respective topographies) were produced. Since each simulation contained one dipole cluster, we produce single source EEG-snapshots.

C. The finite-element-based CNN for EEG inverse source reconstructions

The design and training of the proposed feCNN (see Fig. 1 was accomplished using the Tensorflow [11] and Keras [12] libraries. The proposed network takes as input an EEG topography and predicts the electrical current of each dipole in the source space. Thus, our CNN can be mathematically described as:

$$\Phi : \mathbb{R}^{67\times67} \longrightarrow \mathbb{R}^{10092} \tag{3}$$

The input topography passes through a two-dimensional (2D)-Convolution layer with 8 filters that have a size of 2×2. Furthermore, the output tensor $\mathbf{g} \in \mathbb{R}^{65\times65\times8}$ is flattened in order to traverse three fully connected layers with 1024 neurons each. Before each one these three layers there are also Batch Normalization [13] and Dropout [13] layers. Finally, each neuron of the output layer corresponds to a dipole in the source space and as a result our CNN predicts the amplitude of each dipole.

We experimented with several loss functions for regression problems but we ultimately decided to use the Mean absolute error (MAE) (4) as it allowed a fast convergence of our CNN compared to others. If $\mathbf{y}$ denotes the true values, $\tilde{\mathbf{y}}$ the predicted values and N the length of both the vectors with actual and predicted values, MAE can be mathematically described as [13]:

$$L(\mathbf{y}, \tilde{\mathbf{y}}) = \frac{1}{N}\sum_{i=1}^{N} \left|y_i - \tilde{y}_i\right| \tag{4}$$

Moreover, we opted for Rectified Linear Unit (ReLU) [13] as activation as it have demonstrated superior performance in tests when compared to alternatives.

Finally, convolution filters, weights and biases were optimized using the Stochastic Gradient Descent (SGD) algorithm [13] with a learning rate $\lambda = 0.001$ and batch size of 32.

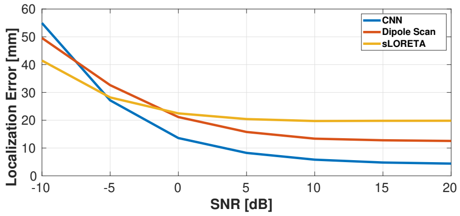

Fig. 2: Localization Error for various SNR levels

The proposed convolutional neural network was trained with $100,000$ simulated sources and their respective topographies over 500 epochs in the Jetson AGX.

III. Evaluation

We now evaluate the performance of our CNN and compare it to state-of-the-art inverse algorithms, namely sLORETA [15] and Singe Dipole Scan [14]. We assessed the performance of the neural network using both simulated and real EEG recordings. The localization error (LE) [16] is used as metric to quantify EEG source localization performance. LE can be quantified as the Euclidean distance between truly activated source r_{true} and the reconstructed peak source r_{peak} in three dimensional source space:

$$\text{LE} = ||r_{\text{true}} - r_{\text{peak}}||_2 \tag{5}$$

A. Evaluation for various SNR levels

We ran simulations with various SNR levels to measure localization accuracy in several actual conditions. While our CNN is trained with 15 dB SNR data, we used SNR levels ranging from -10 dB to 20 dB in the evaluation. For each SNR level, $5,000$ samples (EEG and sources data) were simulated. The localization error for each SNR level is shown in the Fig. 2. Our feCNN outperformed traditional methods at high SNR levels, but performed worse at low SNR levels (< -7.5 dB).

B. Influence of the depth of the simulated source

The effect of the source's depth is investigated. The larger depth of the seed dipole is, the less it influences the EEG signal. Thus, the larger the depth is, the more difficult the localization is. We compared the performance of the inverse methods (feCNN, sLORETA, Single Dipole Scan) for all the depths in the source space and different SNR levels (see Fig. 3). Another finding is that feCNN is capable to correctly localize even deep sources. In particular, while Dipole Scan has the worst localization results and strongly depends on the depth of the source, both feCNN and sLORETA slightly depend on the depth of the source cluster. Furthermore, for all Signal-to-noise ratios, feCNN yields the less localization error over all the spectrum of the depths. Finally, as expected, as the SNR increases the dependence of the localization methods on the depth of the neural source decrease and thereby they yield better results.

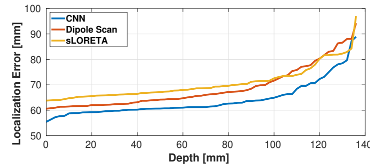

(a) SNR $= -10$dB

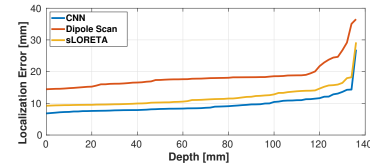

(b) SNR $= 10$dB

Fig. 3: Localization Error for various SNR levels and depths

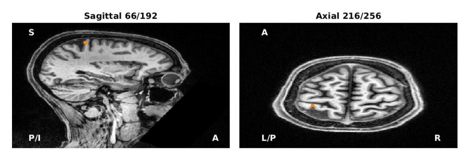

(a) feCNN

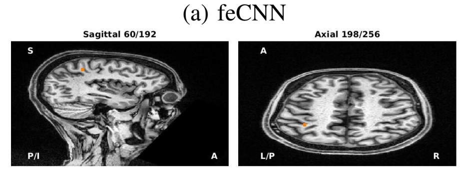

(b) sLORETA

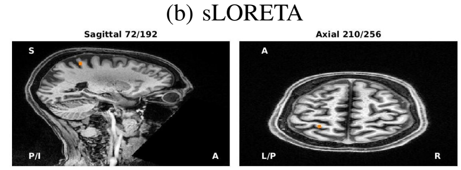

(c) Dipole Scan

Fig. 4: Source Localization with real EEG data

C. Evaluation with real data

To realistically evaluate the performance of feCNN and the other inverse algorithms, we used real EEG recordings. The EEG recordings are from [1] and they can be found here [17]. As described in [1], Somatosensory evoked potentials (SEP) were acquire using 80 AgCl sintered ring electrodes (EASY-CAP GmbH, Herrsching, Germany, 74 EEG channels plus additional six channels to detect eye movements). The median nerve at the right wrist of five right-handed healthy subjects was stimulated with monophasic square-wave electrical pulses having a duration of 0.5 ms.

Having preprocessed with FieldTrip [10] the Somatosensory evoked potentials, we localized them with all the inverse methods. The localizations projected on the MRI of the subject are shown in Fig. 4.

Principally, in real EEG-recordings, as opposed to simulated, we cannot know the location of the dipole cluster that gave rise to the recorded EEG signal. Therefore, we cannot use the localization error to quantify the performance of the inverse methods. However, the EEG-recordings were generated by a very specific experiment with particular parameters and many studies [18], [19] verify that this type of stimulus is localized in the Primary Somatosensory Cortex (S1).

It can be seen from Fig. 4 that both our neural network and Dipole Scan correctly localize the SEP to the S1, while sLORETA estimates inaccurately a deeper location.

IV. Discussion & Future Directions

In this study, we propose a deep learning method, the feCNN, for EEG source localization. Initially, to model realistically the geometrical and electromagnetic features of the head, we solve the forward problem using a six-compartment head model based on [1]. Having calculated the leadfield matrix, we simulate EEG recordings and their respective electric activations in the source space. Moreover, we train feCNN using the electric activations as target data and their corresponding topographies (generated from the EEG simulated signals) as input. Finally, we access the accuracy and robustness of feCNN with both real and simulated EEG data.

Within the limited scope of our experiments, our approach seems to compare very favorably to traditional numerical approaches. The results in the simulated data suggest that feCNN appears reasonably good localizations compared to sLORETA and Single Dipole Scan solutions. Even though feCNN is trained with 15 dB SNR data, it can correctly localize EEG data in a wide range of SNR levels (see Fig. 2). Moreover, by comparison with the sLORETA and Single Dipole Scan methods, is the less dependent and almost independent (for high SNR levels) on the source depth (see Fig. 3). Eventually, feCNN has the generalization ability to correctly localize the somatosensory evoked potentials to S1 (see Fig. 4).

However, our method despite the advantages comes with limitations. First of all, the orientations of the dipoles in the head model are not estimated. Furthermore, our approach is under the assumption that brain activity is always smooth. As a future solution is to generate a proportion of the training data with Random Markov Fields while the rest of them could follow a Gaussian distribution. Moreover, feCNN is not trained to localize EEG data in a distributed dipole model with more than one sources. We intent to expand feCNN in order to resolve this issue if each simulation contains more than one dipole clusters. Finally, our method is not independent of the source space and the anatomy of the brain as it is under the assumption that all source spaces have $10,092$ dipoles.

We now compare feCNN with ConvDip [7], ESBN [9] and DeepMeg [8] in terms of forward modeling and architecture. ConvDip [7] and ESBN [9] use relatively small source spaces with 5124 and 1024 dipoles respectively, while feCNN and DeepMeg [8] have learned to localize data in 10092 and 15002 dipoles respectively. Moreover, feCNN and ESBN [9] solved the forward problem using FEM, whereas ConvDip [7] using BEM and DeepMeg [8] using BrainStorm [20]. All neural networks, except DeepMeg [8] which predicts the location(s) of the electric activation(s), estimate the amplitude of each dipole. Furthermore, DeepMeg [8] and ESBN [9] take as input the channel measurements while feCNN and ConvDip [7] take the topography generated from the EEG electrodes. Finally, feCNN, ConvDip [7] and ESBN [9] have correctly localized real EEG recordings.

We showed that feCNN is capable to localize EEG recordings in a realistic anatomy. Thus, feCNN is a promising inverse solver and with enough future expansions it could potentially pave the way for real-time source localization.

References

[1] M. Antonakakis et al., "The effect of stimulation type, head modeling, and combined EEG and MEG on the source reconstruction of the somatosensory P20/N20 component," Hum. Brain Mapp., vol. 40, no. 17, pp. 5011–5028, 2019.

[2] R. Grech et al., "Review on solving the inverse problem in EEG source analysis," J. Neuroeng. Rehabil., vol. 5, no. 1, p. 25, 2008.

[3] M. Antonakakis, "The effect of experimental and modeling parameters on combined EEG/MEG source analysis and transcranial electric stimulation optimization of somatosensory and epilepsy activity," University of Münster, Münster, 2021.

[4] J. C. de Munck, C. H. Wolters, and M. Clerc, "EEG and MEG: forward modeling," in Handbook of Neural Activity Measurement, R. Brette and A. Destexhe, Eds. Cambridge: Cambridge University Press, 2012, pp. 192–256.

[5] C. H. Wolters, A. Anwander, G. Berti, and U. Hartmann, "Geometry-adapted hexahedral meshes improve accuracy of finite-element-method-based EEG source analysis," IEEE Trans. Biomed. Eng., vol. 54, no. 8, pp. 1446–1453, 2007.

[6] S. Schrader et al., "DUNEuro-A software toolbox for forward modeling in bioelectromagnetism," PLoS One, vol. 16, no. 6, p. e0252431, 2021.

[7] L. Hecker, R. Rupprecht, L. Tebartz Van Elst, and J. Kornmeier, "ConvDip: A convolutional neural network for better EEG source imaging," Front. Neurosci., vol. 15, p. 569918, 2021.

[8] D. Pantazis and A. Adler, "MEG source localization via deep learning," arXiv [eess.SP], 2020.

[9] C. Wei, K. Lou, Z. Wang, M. Zhao, D. Mantini, and Q. Liu, "Edge sparse basis network: A deep learning framework for EEG source localization," in 2021 International Joint Conference on Neural Networks (IJCNN), 2021.

[10] R. Oostenveld, P. Fries, E. Maris, and J.-M. Schoffelen, "FieldTrip: Open source software for advanced analysis of MEG, EEG, and invasive electrophysiological data," Comput. Intell. Neurosci., vol. 2011, p. 156869, 2011.

[11] Martín Abadi et al., Tensorflow: A system for large-scale machine learning. 2015.

[12] F. Chollet, Keras. 2015.

[13] I. Goodfellow, Y. Bengio, and A. Courville, Deep Learning. London, England: MIT Press, 2016.

[14] M. Fuchs et al., "Improving source reconstructions by combining bioelectric and biomagnetic data," Electroencephalogr. Clin. Neurophysiol., vol. 107, no. 2, pp. 93–111, 1998.

[15] R. D. Pascual-Marqui, "Standardized low resolution brain electromagnetic tomography (SLORETA): Technical details" in Methods and findings in experimental and clinical pharmacology, pp. 5–12, 02 2002.

[16] F. Lucka, S. Pursiainen, M. Burger, and C. H. Wolters, "Hierarchical Bayesian inference for the EEG inverse problem using realistic FE head models: depth localization and source separation for focal primary currents", NeuroImage, pp. 1364–1382, 2012.

[17] M. C. Piastra et al., "The WWU DUNEuro reference data set for combined EEG/MEG source analysis." 2020.

[18] A. Nakamura et al., "Somatosensory homunculus as drawn by MEG," Neuroimage, vol. 7, no. 4 Pt 1, pp. 377–386, 1998.

[19] D. van Westen, P. Fransson, J. Olsrud, B. Rosén, G. Lundborg, and E.-M. Larsson, "Fingersomatotopy in area 3b: an fMRI-study," BMC Neurosci., vol. 5, p. 28, 2004.

[20] F. Tadel, S. Baillet, J. C. Mosher, D. Pantazis, and R. M. Leahy, "Brainstorm: a user-friendly application for MEG/EEG analysis," Computational intelligence and neuroscience, 2011.